Contribution from the Department of Chemistry, University of California, Berkeley, California 94720, and Institut für Organische Chemie der Friedrich-Alexander-Universität Erlangen-Nürnberg, D-8520 Erlangen, Federal Republic of Germany

Unusual Structures of Dilithiosilanes and Disodiosilanes. Ionicity of the Silicon–Alkali-Metal Bond

Andrzej Rajca,*[,1a,b] Peng Wang,[1b] Andrew Streitwieser,*[,1b] and Paul von R. Schleyer*[,1c]

Received January 15, 1989

Both dilithiosilanes (SiH_2Li_2) and disodiosilanes (SiH_2Na_2) favor unusual structures. The lowest singlet and lowest triplet potential energy surfaces (PES) were searched with the 3-21G and 3-21G(*) basis sets, and a number of stationary points were located. The "normal" tetrahedral-based singlet, **3s** (C_{2v}), was the lowest energy structure at HF but not at correlated levels of theory. The most interesting singlet SiH_2Li_2 structures were reoptimized at HF/6-31G**, and the final energies were calculated at MP4SDTQ/6-31G** and corrected for the zero-point vibrational energy. In the global minimum structure (**1s**), the lithiums are unsymmetrically placed in the C_s plane orthogonal to the SiH_2 moiety. This form is 6.3 kcal mol^{-1} lower in energy than the conventional tetrahedral singlet (**3s**) and 3.9 kcal mol^{-1} lower than the inverted tetrahedral singlet (**2s**). The $^3B_2$ state with a conventional tetrahedral geometry, lying only 14.1 kcal mol^{-1} above **1s** at UMP2/6-31G*//3-21G(*) + ZPVE, is the lowest triplet **1t**. Other local triplet minima include **2t** ($^3A''$, C_s) with all atoms in the same plane, **3t** ($^3B_2$) with an inverted tetrahedral structure, **4t** ($^3A'$) with a structure similar to **1s**, and **5t** ($^3B_1$, C_{2v}) with collinear SiLiLi. The triplets **2t**, **3t**, **4t**, and **5t** are 15.0, 18.0, 20.8, and 25.8 kcal mol^{-1}, respectively, above the global singlet minimum. Some of the corresponding energy minima were calculated for disodiosilanes at 3-21G. The ionicity of the SiLi and SiNa bonds is compared to that of the CLi and CNa bonds by means of NPA and integrated projected electron population analyses.

Introduction

Organolithium compounds favor unusual structures, particularly when more than one lithium is present.[2] For example, dilithiomethane, CH_2Li_2, is nearly degenerate for the planar and tetrahedral tetracoordinate carbon.[2–4] Interest in the phenomenon is not limited to inorganic and organometallic chemistry, since the synthesis of a hydrocarbon with potentially planar tetracoordinate carbon has been a challenging endeavor.[5] We now report a calculational examination of SiH_2Li_2 and provide comparisons with SiH_2Na_2. The structures of CH_2Li_2,[2,3b,4] SiH_3Li,[6] and $SiLi_4$[7] serve as prototypes. The C–Li bond in singlet dilithiomethane is predominantly ionic; this results in near degeneracy of the tetrahedral and planar arrangements of the two lithium cations and the methylene dianion.[3b,4] Triplet CH_2Li_2, which can be considered approximately to comprise a methylene radical anion and a dilithium radical cation,[4b] behaves similarly in this sense. The possibility that silicon also might exhibit planar instead of tetrahedral coordination is receiving increasing attention.[8,9] While π-donor–σ-acceptor substituents have been shown to be effective in this context,[8] the influence of strong σ-donor groups (i.e., those with the opposite polarity) has been only partially explored.[7,8]

Another structural aspect of silanes is the highly polar character of the Si–H bonds and the hydridic character of the hydrogens. Hence, geometries in which the alkali-metal cations interact electrostatically with the negatively charged hydrogens may be competitive with more conventional structures in which the cations interact with silicon. Indeed, an inverted tetrahedral structure (C_{3v} symmetry) is the global minimum on the silyllithium, SiH_3Li, potential energy surface.[6] Tetralithiosilane, $SiLi_4$, also prefers an inverted (C_{2v}) rather than a tetrahedral (or a planar) structure.[7] The present calculation achieves added significance from recent evidence for the formation of dilithiodimesitylsilane in solution.[10]

Computational Methods

All calculations were carried out with the standard 3-21G, 3-21G(*), 6-31G*, and 6-31G** basis sets. The d exponent of silicon was 0.45, and the p exponent of hydrogen was 1.2 (6-31G**).[9c,11] Møller–Plesset (MP2, MP3, and full-fourth-order MP4) perturbation theory was employed for the electron correlation corrections.[12] Harmonic vibrational frequencies and zero-point energies (3-21G//3-21G) were obtained from analytical second derivatives and scaled by 0.9.[13] RHF and UHF were used for calculations of the singlets and triplets, respectively. The calculations were carried out with various versions of the GAUSSIAN series of programs on a VAX-750 at Berkeley and a CONVEX at Erlangen.[14] Projected electron density functions were calculated by using the program PROJ,[15] and the numerical "integrated projected electron population", IPP, integrations were carried out for regions bounded by minima in the pro-

(1) (a) Miller Fellow, 1985–87; permanent address: Department of Chemistry, Kansas State University, Manhattan, KS 66506. (b) University of California. (c) University of Erlangen-Nürnberg.

(2) Schleyer, P. v. R. *Pure Appl. Chem.* **1983**, *55*, 355; **1984**, *56*, 151. Maercker, A.; Theis, M. *Top. Curr. Chem.* **1987**, *138*, 1. Setzer, W. N.; Schleyer, P. v. R. *Adv. Organomet. Chem.* **1985**, *24*, 354. Schade, C.; Schleyer, P. v. R. *Ibid.* **1987**, *27*, 169. Ritchie, J. P.; Bachrach, S. W. *J. Am. Chem. Soc.* **1987**, *109*, 5909.
(3) (a) Kawa, H.; Manley, B. C.; Lagow, R. J. *J. Am. Chem. Soc.* **1985**, *107*, 5313. (b) Collins, J. B.; Dill, J. D.; Jemmis, E. D.; Apeloig, Y.; Schleyer, P. v. R.; Seeger, R.; Pople, J. A. *J. Am. Chem. Soc.* **1976**, *98*, 5419. (c) Hoffmann, R.; Alter, R. W.; Wilcox, C. F., Jr. *J. Am. Chem. Soc.* **1970**, *92*, 4992.
(4) (a) Laidig, W. D.; Schaefer, H. D., III. *J. Am. Chem. Soc.* **1978**, *100*, 5972. (b) Bachrach, S. W.; Streitwieser, A., Jr. *J. Am. Chem. Soc.* **1984**, *106*, 5818. (c) Alvarado-Swaisgood, A. E.; Harrison, J. F. *J. Phys. Chem.* **1985**, *89*, 62. (d) Sen, K. D.; Boehm, M. C.; Schmidt, P. C. *THEOCHEM* **1984**, *15*, 271.
(5) Venkatachalam, M.; Jawdosiuk, M.; Deshpande, M.; Cook, J. M. *Tetrahedron Lett.* **1985**, *2275*. Keese, R.; Pfenninger, A.; Roesle, A. *Helv. Chim. Acta* **1979**, *62*, 326. Dietrich, H.; Mahdi, W.; Storch, W. J. *J. Organomet. Chem.* **1988**, *349*, 1. Harder, S.; Boersma, J.; Brandsma, L.; van Heteren, A.; Kanters, J.; Bauer, W.; Schleyer, P. v. R. *J. Am. Chem. Soc.* **1988**, *110*, 7802.
(6) Schleyer, P. v. R.; Clark, T. *J. Chem. Soc., Chem. Commun.* **1986**, 1371.
(7) Schleyer, P. v. R.; Reed, A. *J. Am. Chem. Soc.* **1988**, *110*, 4453.
(8) Aldoshin, S. M.; D'yachenko, O. A.; Atovmyan, L. O.; Chekhlov, A. I.; Al'yanov, M. I. *Koord. Khim.* **1980**, *6*, 936. Meyer, H.; Nagorsen, G. *Angew. Chem., Int. Ed. Engl.* **1979**, *18*, 551. Dunitz, J. D. *Angew. Chem., Int. Ed. Engl.* **1980**, *19*, 1034.
(9) (a) Würthwein, E. U.; Schleyer, P. v. R. *Angew. Chem., Int. Ed. Engl.* **1979**, *18*, 553. (b) Krogh-Jespersen, M. B.; Chandrasekhar, J.; Würthwein, E. U.; Collins, J. B.; Schleyer, P. v. R. *J. Am. Chem. Soc.* **1980**, *102*, 2263. (c) Hehre, W. J.; Radom, L.; Schleyer, P. v. R.; Pople, J. A. *Ab Initio Molecular Orbital Theory*; Wiley: New York, 1986; p 428.
(10) West, R. Personal communication.
(11) Gordon, M. S.; Binkley, J. S.; Pople, J. A.; Pietro, W. J.; Hehre, W. J. *J. Am. Chem. Soc.* **1982**, *104*, 2797. Francl, M. M.; Pietro, W. J.; Hehre, W. J.; Binkley, J. S.; Gordon, M. S.; DeFrees, D. J.; Pople, J. A. *J. Chem. Phys.* **1982**, *77*, 3655. Hehre, W. J.; Ditchfield, R.; Pople, J. A. *J. Chem. Phys.* **1972**, *56*, 2251. Dill, J. D.; Pople, J. A. *J. Chem. Phys.* **1975**, *62*, 2921. Hariharan, P. C.; Pople, J. A. *Theor. Chim. Acta* **1973**, *28*, 213.
(12) Pople, J. A.; Binkley, J. S.; seeger, R. *Int. J. Quantum Chem., Symp.* **1976**, *10*, 1. Binkley, J. S.; Pople, J. A. *Ibid.* **1975**, *9*, 229 and references therein.
(13) Pople, J. A.; Schlegel, H. B.; Krishnan, R.; DeFrees, D. J.; Binkley, J. S.; Frisch, M. J.; Whiteside, R. A.; Hout, R. F., Jr.; Hehre, W. J. *Int. J. Quantum Chem., Symp.* **1981**, *15*, 269. DeFrees, D. J.; McLean, A. D. *J. Chem. Phys.* **1985**, *82*, 333. Also see: Komornicki, A.; Pauzat, F.; Ellinger, Y. *J. Phys. Chem.* **1983**, *87*, 3847.
(14) Binkley, J. S.; Frisch, M. J.; DeFrees, D. J.; Raghavachari, K.; Whiteside, R. A.; Schlegel, H. B.; Fluder, E. M.; Pople, J. A. "GAUSSIAN 82"; Carnegie-Mellon University Publication Unit: Pittsburgh, PA, 1983. Binkley, J. S.; Whiteside, R. A.; Krishnan, R.; Seeger, R.; DeFrees, D. J.; Schlegel, H. B.; Topiol., S.; Kahn, L. R.; Pople, J. A. *QCPE* **1981**, *13*, 406.
(15) Collins, J. B.; Streitwieser, A., Jr.; McKelvey, J. M. *J. Comput. Chem.* **1979**, *3*, 79.

Table I. Total Energies[a] for Dilithiosilanes[b,c]

species	sym	elec state	3-21G //3-21G	3-21G(*) //3-21G(*)	6-31G* //3-21G(*)	MP2/6-31G* //3-21G(*)
1s	C_s	$^1A'$	303.318 70 (0)	303.389 52	304.926 74	305.040 63
2s	C_{2v}	$^1A_1$	303.314 45 (0)[b]	303.381 94[b]	304.919 28	305.034 44
3s	C_{2v}	$^1A_1$	303.323 65 (0)	303.392 02	304.927 53	305.033 64
1s*	C_s	$^1A'$	303.313 73 (1)	303.382 10 (1)	304.919 52	305.031 08
2s*	C_s	$^1A'$	303.316 22 (1)	303.386 74	304.923 47	305.033 92
4s	C_{2v}	$^1A_1$	303.290 58 (3)[b]	303.357 18[b]	304.892 63	305.001 56
5s	C_{2v}	$^1A_1$	303.306 75 (2)	303.373 55	304.908 93	305.016 09
6s	D_{2h}	^1A_g	303.151 56 (2)	303.263 76		
3s*	C_s	$^1A'$	303.265 96 (1)	303.340 04		
1t	C_{2v}	$^3B_2$	303.327 99 (0)	303.399 37	304.935 80	305.017 92
	C_{2v}	$^3A_2$	303.273 46 (0)			
	C_{2v}	$^3B_1$	303.230 03			
2t	C_s	$^3A''$	303.326 41 (0)	303.396 19	304.932 35	305.016 45
3t	C_{2v}	$^3B_2$	303.309 92 (0)	303.381 94	304.919 28	305.009 42
4t	C_s	$^3A'$	303.312 70 (0)	303.385 60	304.921 93	305.006 31
5t	C_{2v}	$^3B_1$	303.313 51 (0)	303.383 38	304.919 76	304.998 33
6t	C_{2v}	$^3B_1$	303.319 49 (2)	303.388 54	304.924 69	305.007 83
7t	C_{2v}	$^3B_1$	303.309 07			
	C_{2v}	$^3A_2$	303.271 92			
$Li_2 + H_2Si$		($^1A_1$)	303.253 54[b]	303.329 52[b]		
HLi + HLiSi		($^1A_1$)	303.236 36[b]	303.348 73[b]		
$H_2 + Li_2Si$		($^1A_1$)	303.260 88[b]	303.310 61		
$Li_2 + H_2Si$		($^3B_1$)	303.250 15[b]	303.322 88[b]		
HLi + HLiSi		($^3B_1$)	303.273 43[b]	303.384 01[b]		
$H_2 + Li_2Si$		($^3B_1$)	303.302 66[b]	303.351 71[b]		

[a] Total energies are in –au. [b] *The Carnegie-Mellon Quantum Chemistry Archive*, 3rd ed.; Whiteside, R. A., Frish, M. J., Pople, J. A., Eds.; Carnegie-Mellon University: Pittsburgh, PA, 1983. Luke, B. T.; Pople, J. A.; Krogh-Jespersen, M.-B.; Apeloig, Y.; Chandrasekhar, J.; Schleyer, P. v. R. *J. Am. Chem. Soc.* **1986**, *108*, 260. [c] The number of imaginary frequencies is given in parentheses.

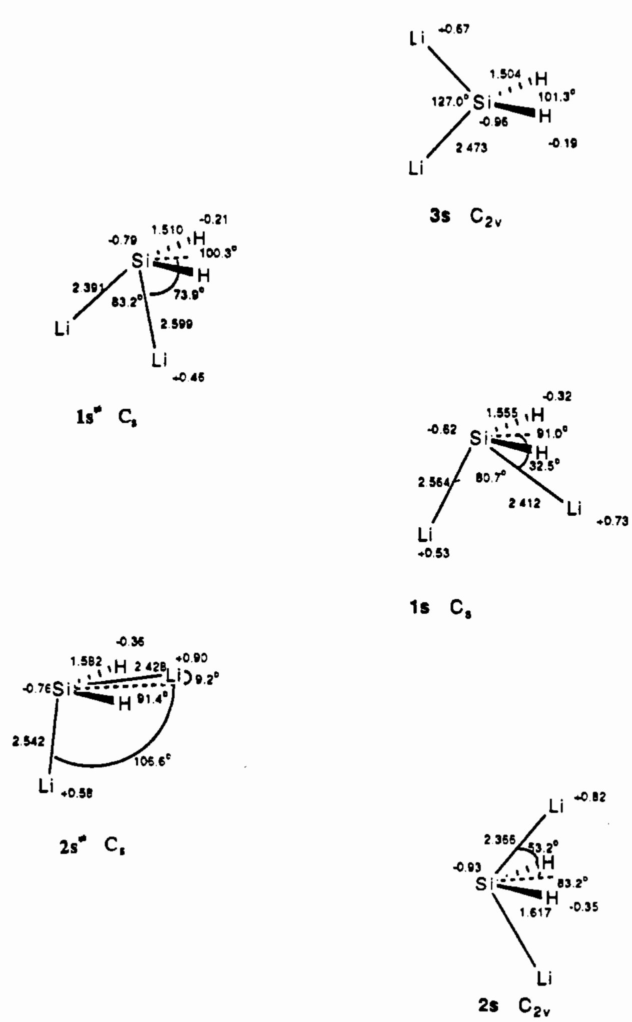

Figure 1. Optimized 6-31G** geometries of **1s***, **2s**, **2s***, and **3s** and optimized MP2/6-31G** geometries of **1s**. The natural atomic charges are calculated at 6-31G**. Bond distances are in angstroms, and bond angles, in degrees.

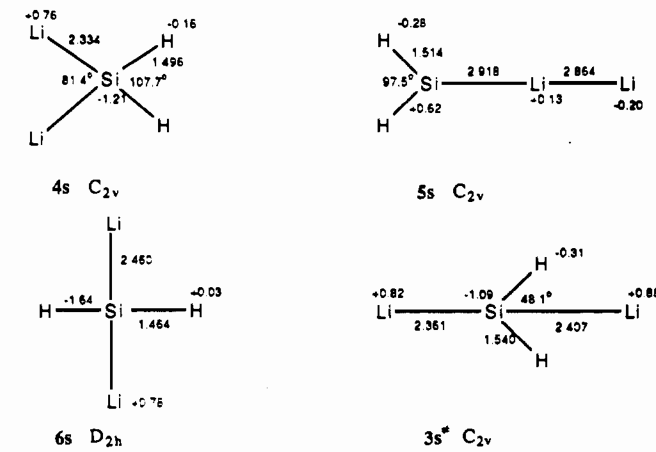

Figure 2. Optimized 3-21G(*) geometries of singlet dilithiosilanes. The natural atomic charges are calculated at 3-21G(*). Bond distances are in angstroms, and bond angles, in degrees.

jected density functions.[16] The minimum-density demarkations of such projected functions are approximations to the zero-flux surface boundaries of Bader;[17] these boundaries are vertical curtains compared to the true zero-flux curved surfaces. Accordingly, the derived integrated populations are only approximations to the three-dimensional integrations over Bader "basins"; however, they have been shown to be qualitatively correct for bonds to silicon and are faster to compute.[18] In addition, the natural population analysis (NPA) of Reed, Weinstock, and Weinhold was also employed.[19]

Results and Discussion

Singlet Dilithiosilanes, SiH_2Li_2. Nine stationary points were located on the singlet dilithiosilane potential energy surface at

(16) McDowell, R. S.; Grier, D. L.; Streitwieser, A., Jr. *Comput. Chem.* **1985**, *9*, 165.
(17) Bader, R. F. W. *Acc. Chem. Res.* **1975**, *8*, 34; **1985**, *18*, 9. Bader, R. F. W.; MacDougall, P. J. *J. Am. Chem. Soc.* **1985**, *107*, 6788. Biegler-Koenig, F. W.; Bader, R. F. W.; Tang, T. H. *J. Comput. Chem.* **1982**, *3*, 317.
(18) Gronert, S.; Glaser, R.; Streitwieser, A. *J. Am. Chem. Soc.*, in press.
(19) Reed, A. E.; Weinstock, R. B.; Weinhold, F. *J. Chem. Phys.* **1985**, *83*, 735.

Table II. Relative Energies and Dipole Moments of Dilithiosilanes[a]

species	elec state	3-21G //3-21G	3-21G* //3-21G(*)	6-31G* //3-21G(*)	MP2/6-31G* //3-21G(*)	ZPVE[b]	MP2/6-31G* //3-21G(*) + ZPVE	μ[c]
1s	$^1A'$	0.0	0.0	0.0	0.0	9.1	0.0	6.26
2s	$^1A_1$	2.7	4.8	4.7	3.9	7.7	2.5	7.15
3s	$^1A_1$	−3.1	−1.6	−0.5	4.4	9.2	4.5	5.99
1s‡	$^1A'$	3.1	4.6	4.5	6.0	8.3	5.2	5.85
2s‡	$^1A'$	1.6	1.7	2.0	4.2	8.7	3.8	6.22
4s	$^1A_1$	17.6	20.3	21.4	24.5	8.2	23.6	7.17
5s	$^1A_1$	7.5	10.0	11.2	15.4	8.9	15.2	0.22
6s	^1A_g	104.9	78.9			7.7		0.0
3s‡	$^1A'$	33.1	31.0			8.2		4.75
1t	$^3B_2$	−5.8	−6.2	−5.7	14.2	9.0	14.1	1.83
	$^3A_2$	28.4						5.39
	$^3B_1$	55.6						−3.52
2t	$^3A''$	−4.8	−4.2	−3.5	15.2	8.9	15.0	
3t	$^3B_2$	5.5	4.8			7.5	18.0	
4t	$^3A'$	3.8	2.4	3.0	21.5	8.4	20.8	
5t	$^3B_1$	3.2	3.8	4.4	26.5	8.4	25.8	12.26
6t	$^3B_1$	−0.5	0.6	1.3	20.6	8.3	19.8	1.91
7t	$^3B_1$	6.0						
	$^3A_2$	29.4						
$Li_2 + H_2Si$	($^1A_2$)			40.9	37.6			
HLi + HLiSi	($^1A_1$)		51.7	25.6				
$H_2 + Li_2Si$	($^1A_1$)		36.3	49.5				
$Li_2 + H_2Si$	($^3B_1$)			43.0	41.8			
HLi + HLiSi	($^3B_1$)		28.4	3.4				
$H_2 + Li_2Si$	($^3B_1$)		10.1	23.7				

[a] Relative energies are in kcal mol^{-1}. [b] Zero-point vibration energies (in kcal mol^{-1}) were calculated at 3-21G//3-21G and scaled by 0.9. [c] Dipole moments are in debyes, calculated at 3-21G//3-21G.

Table III. Total Energies[a] for Dilithiosilanes at Higher Theoretical Levels

species	sym	6-31G** //6-31G**	MP2/6-31G** //6-31G**	MP3/6-31G** //6-31G**	MP4/6-31G** //6-31G**
1s	C_s	304.929 82	305.057 41	305.078 93	305.087 29
2s	C_{2v}	304.922 29	305.050 99	305.071 08	305.078 86
3s	C_{2v}	304.930 85	305.049 84	305.070 11	305.077 23
	C_{2v}[b]	304.930 56	305.049 99	305.070 32	305.077 40
1s‡	C_s	304.926 33	305.048 81	305.069 88	305.077 79
2s‡	C_s	304.923 02	305.048 83	305.069 50	305.077 34

[a] Total energies are in −au. [b] The geometry was optimized at MP2(FU)/6-31G**. FU stands for full-electron correlation.

Table IV. Relative Energies[a] for Dilithiosilanes at Higher Theoretical Levels

species	sym	6-31G** //6-31G**	MP2/6-31G** //6-31G**	MP3/6-31G** //6-31G**	MP4/6-31G** //6-31G**	MP4/6-31G** //6-31G** + ZPVE[b]
1s	C_s	0.00	0.00	0.00	0.00	0.0
2s	C_{2v}	4.72	4.03	4.93	5.29	3.9
3s	C_{2v}	−0.65	4.75	5.53	6.31	6.4
	C_{2v}[c]	−0.46	4.66	5.40	6.21	6.3
1s‡	C_s	2.19	5.40	5.68	5.96	5.2
2s‡	C_s	4.27	5.38	5.92	6.24	5.8

[a] Total energies are in kcal mol^{-1}. [b] Zero-point vibration energies were calculated at 3-21G//3-21G and scaled by 0.9. [c] The geometry was optimized at MP2(FU)/6-31G**.

both the 3-21G and 3-21G(*) levels (Figure 2, Tables I, II). The lowest energy singlet structures, **1s**, **2s**, **3s**, **1s‡**, and **2s‡**, were reoptimized at 6-31G**, and **3s** also was reoptimized at MP2/6-31G** (Figure 1, Tables III, IV). Since this correlated optimization did not alter either the geometry or the relative energy significantly, further refinement at this level was not undertaken.

The normal tetrahedral structure **3s** is a local minimum (all frequencies real at the 3-21G level). Structure **1s** is remarkable: the two lithiums lie in the C_s symmetry plane and on the same side of the HSiH plane. At MP2/6-31G*//3-21G(*) + ZPE, **1s** is 4.5 kcal mol^{-1} lower in energy than **3s**. Transition state **1s‡** connects **3s** and **1s** with a barrier of 5.2 kcal mol^{-1} from **1s**. The inverted C_{2v} structure **2s** also is a local minimum, 2.5 kcal mol^{-1} higher in energy than **1s**. The transition state **2s‡** bridges **1s** and **2s**. Thus, at the MP2/6-31G*//3-21G(*) + ZPE level, the three minima, **3s**, **1s**, and **2s**, interconvert via the transition structures **1s‡** and **2s‡**. This exchange process corresponds to rotating the LiSiLi fragment of the molecule around the H–Si–H fragment with a barrier of less than 5.2 kcal mol^{-1}. The final energies of all of these species were calculated at the MP4SDTQ/6-31G**//6-31G** level, with corrections for zero-point energies. At this level, **1s** is the global singlet SiH_2Li_2 minimum, 6.4 and 3.9 kcal mol^{-1} more stable than **3s** and **2s**, respectively. The transition state **2s‡** between **1s** and **2s** has a barrier of only 1.9 kcal mol^{-1} from **2s**. The energies of **3s** and **1s‡** are nearly the same (Table IV), and the stability order of **3s** and **1s‡** varies with the electron correlation level. With reoptimization of **3s** at full MP2/6-31G**, it is more stable than **1s‡** at MP3/6-31G** but less stable than **1s‡** at MP4/6-31G**. Thus, the characters of the **3s** and **1s‡** stationary points are not fully determined, but the PES in this region must be rather flat. All of these species are 25–50 kcal mol^{-1} more stable at 3-21G(*)//3-21G(*) than the fragments $Li_2 + H_2Si$ ($^1A_1$), HLi + HLiSi ($^1A_1$), and $H_2 + Li_2Si$ ($^1A_1$).

The sequence of structures is also characterized by corresponding changes in structural parameters. As shown in Figure 1, Si–H bond lengths increase along the following series: **3s**, 1.504 Å; **1s***, 1.510 Å; **1s**, 1.555 Å; **2s***, 1.582 Å; and **2s**, 1.617 Å. Correspondingly, the HSiH angles decrease: **3s**, 101°; **1s***, 100°; **1s**, 91°; **2s***, 91°; **2s**, 83°. NPA shows that cationic lithiums and hydridic hydrogens attract each other electrostatically. Indeed, **2s** may be regarded as a symmetrical triple ion between two lithium cations and silylene dianion. It is instructive to consider how the other structures may be rationalized by an ionic model. As pointed out by Schleyer and Reed,[7] a point charge ionic model for $SiLi_4$ leads to tetrahedral symmetry rather than the calculated C_{2v} global minimum. Similarly, a point charge model for SiH_2Li_2 would require C_{2v} symmetry with equivalent lithiums. The observed structures, however, are readily rationalized if the silicon is treated as a polarizable unit. In $SiLi_4$, the charge on silicon would be polarized toward the lithium cations and favor a structure electrostatically with all four lithiums on the same side of a plane containing the silicon. In silylene dianion, however, the silicon charge is polarized away from the hydridic hydrogens. The electrostatic potential of the negative hydrogens favors placing the lithium cations on the hydrogen side of the silicon, as in **2s**, but the electrostatic potential associated with the induced dipole on silicon favors putting the lithiums on the opposite side, as in **3s**. With equivalent lithiums in C_{2v} structures, however, the role of such an induced dipole is minimized. In a structure such as **1s**, on the other hand, one lithium benefits from proximity to the negative hydrogens and the other benefits from the favorable polarization at silicon.

The tricoordinate planar structure **3s***, 31.0 kcal mol^{-1} above **1s** at 3-21G(*)//3-21G(*), is a transition state, corresponding to exchange of the two lithiums in **3s**. The three planar tetracoordinate silicon structures, **4s**, **5s**, and **6s**, are not minima; they have three, two, and two imaginary frequencies, respectively. The cis structure **4s** is 10.3 kcal mol^{-1} less stable than **5s** and 58.6 kcal mol^{-1} more stable than **6s** at 3-21G(*)//3-21G(*).

Triplet Dilithiosilanes. Five local minima were found in the lowest triplet PES at UHF/3-21G (Figure 3). The most stable form is **1t**-$^3B_2$ with the conventional tetrahedral structure. It is only 14.1 kcal mol^{-1} above **1s** at UMP2/6-31G*//3-21G(*) + ZPVE. A remarkable C_s minimum, **2t**-$^3A''$, in which all atoms are in the same plane but all bonds to silicon are somewhat different, lies only 0.9 kcal mol^{-1} above **1t**-$^3B_2$. This $^3A''$ structure is an example of planar tetracoordinate silicon. None of the other structures (singlet or triplet) with planar tetracoordinate silicon arrangements is a local minimum. The C_{2v} structure, **3t** ($^3B_2$), is of interest because the hydrogens and lithiums are all on the same side of silicon. This structure is the triplet analogue of **2s**; however, the Li–Li bond in **3t** is only 2.36 Å, compared to 3.51 Å in **2s**. The latter structure was considered simply as a triple ion with the lithiums as cations. In **3t** there is clearly substantial lithium–lithium bonding. For comparison, the bond length of Li_2 is 2.67 Å and that of Li_2^+ is 3.17 Å at 6-31G*.[18] The local minimum, **4t**-$^3A''$, which is 6.6 kcal mol^{-1} above **1t**-$^3B_2$, has a geometry similar to **1s** and can be considered to be a distorted **1t**-$^3B_2$ structure with both lithiums in the C_s plane but on the same side of the SiH_2 plane. In **5t**-$^3B_1$, all atoms are coplanar and the silicon and the lithiums are collinear; it is higher in energy than **1t** by 11.6 kcal mol^{-1}. This section of the PES is exceedingly flat; the two lowest harmonic vibrational frequencies (HF/3-21G) for **5t**-$^3B_1$ are only 57.0 (B_2) and 60.8 cm^{-1} (B_1) (all the other triplets have frequencies greater than 190 cm^{-1}). Actually, the B_2 and B_1 modes correspond to the reaction coordinates, leading to the **2t**-$^3A''$ and the **1t**-$^3B_2$ structures, respectively. The triplet planar cis structure (**6t**-$^3B_1$), only 5.5 and 4.7 kcal mol^{-1} above **1t**-$^3B_2$ and **2t**-$^3A''$, respectively, possesses two imaginary frequencies: 233*i* (A_2) and 149*i* cm^{-1} (B_2). The A_2 and B_2 modes correspond to distortion of the **1t**-$^3B_2$ and **2t**-$^3A''$ structures, respectively. Consequently, the barrier for the rearrangement of **1t**-$^3B_2$ to **2t**-$^3A''$ should be less than 4.7 kcal mol^{-1} at this level of theory.

At the Hartree–Fock level the stability of the triplets is overestimated relative to that of the singlets.[20] The 3-21G relative energies (relative to **3s**) for the tetrahedral triplet (**1t**) and the planar triplet, cis (6t), are −2.7 and 2.6 kcal mol^{-1}, respectively, but become 11 and 18 kcal mol^{-1}, respectively, at MP2/6-31G*//3-21G(*). For comparison, the values for corresponding dilithiomethanes are −16 and −13 kcal mol^{-1}, respectively, at 4-31G, and 4.7 and 5.9 kcal mol^{-1}, respectively, at the DZ + P/CI level.[3b,5a] The five minima are more than 20 kcal mol^{-1} more stable than Li_2 + H_2Si ($^3B_1$) and H_2 + Li_2Si ($^3B_1$) at 3-21G(*)//3-21G(*) but have stability similar to that of HLi + HLiSi ($^3B_1$) at this level of theory.

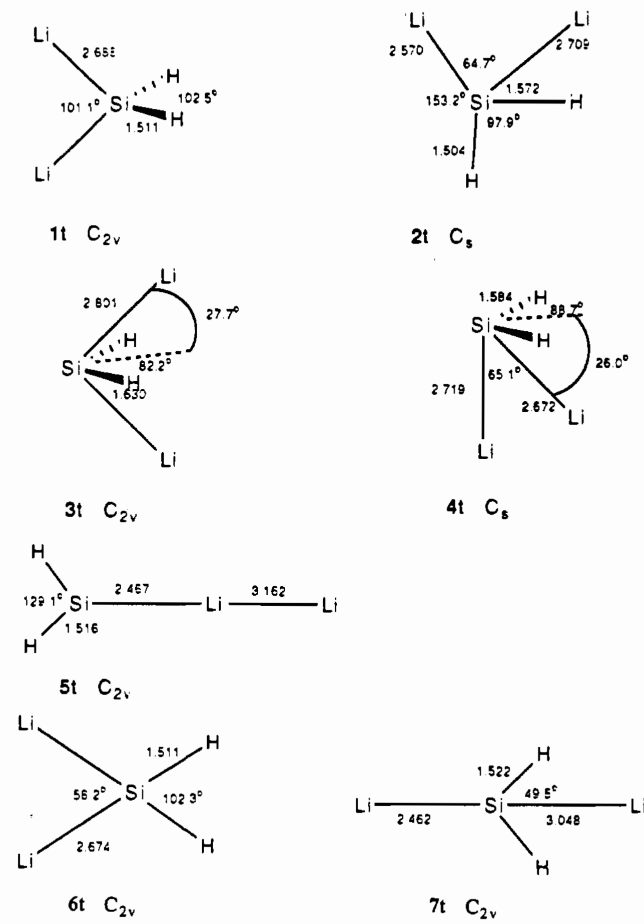

Figure 3. Optimized 3-21G geometries of triplet dilithiosilanes. Bond distances are in angstroms, and bond angles, in degrees.

In general, the changes from the singlet states to the lowest triplet states can be rationalized by promotion of an electron from the HOMO of the singlet, essentially a silicon p lone pair perpendicular to the H–Si–H plane, to the a_1 LUMO, which is mostly a metal–metal σ bond. The lowest triplets may be regarded as a silylene radical anion associated with a dilithium radical cation. It is interesting to consider three triplet states, $^3B_2$, $^3A_2$, and $^3B_1$, for tetrahedral dilithiosilane (Table II, Figure 5) in this context. The lowest energy form of the three, the **1t**-$^3B_2$ state, is formed by promotion of one electron from the b_2 HOMO to the a_1 LUMO; the latter is mostly Li–Li π-bonding (lithium p_x and s) with a significant contribution from the lithium p_z orbitals. More importantly, the s and p_z orbitals dominate the a_1 HOMO of the triplet and form an out-of-phase combination on the silicon side of the Li–Li bond axis and an in-phase combination on the other side. This shift of the electron density from the a_1 HOMO of the triplet on the outside of the Li–Li bond axis results in a greatly reduced dipole moment for the $^3B_2$ state, compared to the cor-

(20) The singlet–triplet energy differences for CH_2 are calculated to be 30.8 kcal mol^{-1} (6-31G*//6-31G*) and 20.9 kcal mol^{-1} (MP2/6-31G*); see ref 7b. The highest levels of theory predict a value in agreement with the experimental value, 9.05 kcal mol^{-1}. See: McKellar, A. R. W.; Bunker, P. R.; Sears, T. J.; Evenson, K. M.; Saykally, R. J.; Langhoff, S. R. *J. Chem. Phys.* **1983**, *79*, 5251.

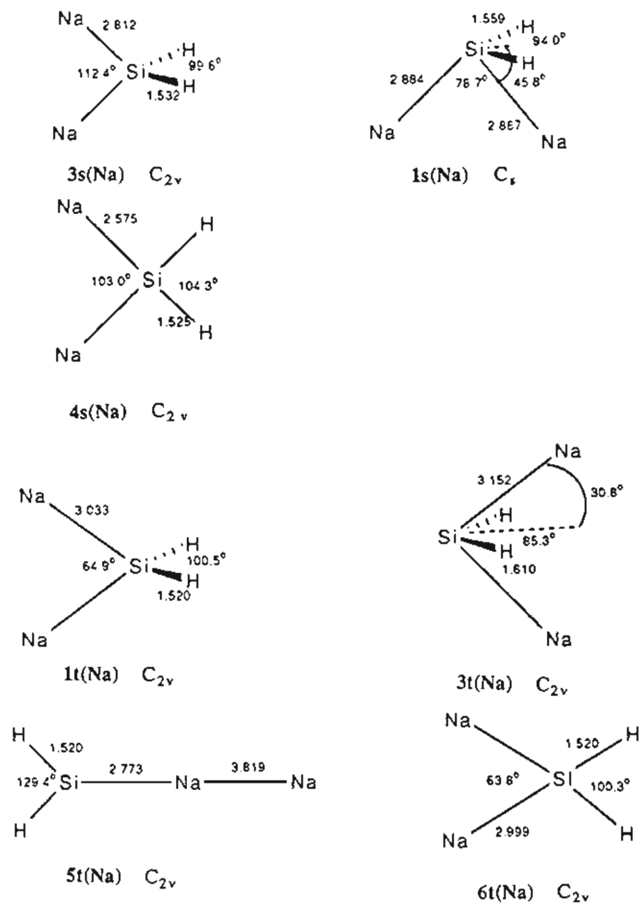

Figure 4. Optimized 3-21G geometries of disodiosilanes. Bond distances are in angstroms, and bond angles, in degrees.

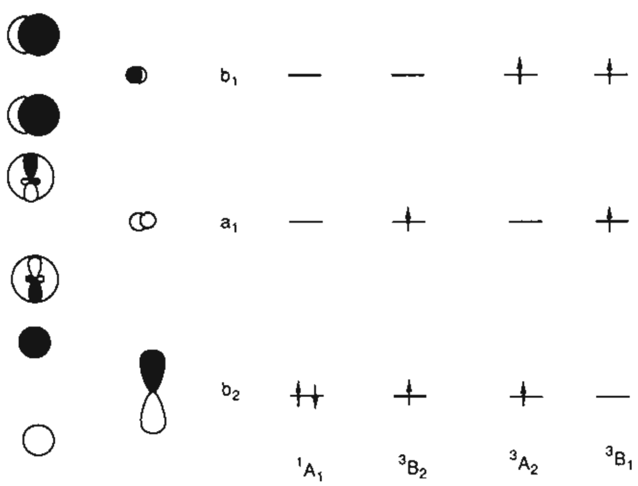

Figure 5. Selected molecular orbitals (b_2, a_1, and b_1) for singlet "tetrahedral" dilithiosilane at 3-21G and their electronic occupations in different triplet states for tetrahedral geometry. The orbital lobes are drawn in the $SiLi_2$ plane (zx) and only contributions from Si (on the right) and Li (on the left) are shown.

responding singlet (Table II). The population of the orbital localized mostly over the lithiums causes only a small reduction in the dipole moment; note the example shown by the $^3A_2$ state. The $^3A_2$ state, a minimum, is 34.2 kcal mol^{-1} above $^3B_2$ (HF/3-21G; Tables I and II) and is formed by promotion of one electron from the b_2 HOMO of the singlet to the b_1 MO. This b_1 MO is essentially a Li–Li π MO perpendicular to the LiSiLi plane and consists largely of highly diffuse Li p_y orbitals. The changes in molecular geometry compared to the singlet are less than those for the $^3B_1$ state; the Li–Li and Si–Li distances are 2.957 and 2.586 Å, respectively. The dipole moment remains practically unchanged from the singlet. Finally, when one of the two electrons in the b_2 HOMO is placed in the a_1 LUMO and the other in the higher b_1 MO, the resulting $^3B_3$ state (61.4 kcal mol^{-1} higher than $^3B_2$ (HF/3-21G)) has the character of a singlet silylene associated with a triplet dilithium. The dipole moment acquires a positive direction (toward the hydrogens), the Si–Li distances increase to 3.396 Å, and the Li–Li distance decreases to 2.541 Å.

As mentioned above, the low-lying triplets, **1t**-$^3B_2$ and **6t**-$^3B_1$, can be viewed as complexes of a silylene anion radical with a dilithium cation radical. The other low-lying triplets also have this feature. In **2t**-$^3A''$, one of the lithiums of the dilithium radical cation interacts with one of the hydridic hydrogens (vide infra); the Li–Li distance increases from 2.600 Å for **6t**-$^3B_1$ to 2.828 Å for **2t**-$^3A''$, and one of the Li–H distances is only 1.923 Å (Figure 3). Thus, **2t**-$^3A''$ also has some character pertaining to a complex of a triplet silylene, HLiSi, and a lithium hydride, LiH. **4t**-$^3A'$ is an analogous compromise between Li–Li bonding and Li–H bridging. The lithiums, which are separated by 2.900 Å, are within the C_s plane orthogonal to the SiH_2 plane. One of the lithiums possesses a close contact, 2.056 Å, to both hydrogens. The collinear arrangement of the silicon and the lithiums is attained in **5t**-$^3B_1$ (Figure 3). Consequently, the dilithium cation radical in **5t** is both charge and spin polarized, approaching the limit of the triplet pair of a H_2SiLi radical and a lithium atom. The large polarizability of silicon is probably an important factor in the stabilization of **5t**-$^3B_1$.

Table V. Total[a] and Relative Energies[b] for Disodiosilanes

species	sym	elec state	3-21G //3-21G	rel energies 3-21G
3s(Na)	C_{2v}	$^1A_1$	610.242 66	0.0
1s(Na)	C_s	$^1A_1$	610.238 82	2.4
4s(Na)	C_{2v}	$^1A_1$	610.204 92	23.7
1t(Na)	C_{2v}	$^3B_2$	610.252 03	−5.9
3t(Na)	C_{2v}	$^3B_2$	610.237 91	3.0
5t(Na)	C_{2v}	$^3B_1$	610.241 48	0.7
6t(Na)	C_{2v}	$^3B_1$	610.244 93	−1.4

[a] Total energies are in −au. [b] Relative energies are in kcal mol^{-1}.

Table VI. Integrated Projected Electron Population (IPP) for Lithium and Sodium

	IPP, e		
	3-21G	6-31G*	P_{min}[a]
SiH_3Li	2.167	2.185	0.083
SiH_3Na	10.228		
CH_3Li[b]		2.134	0.126
SiH_2Li_2 (3s)	2.237	2.241	0.083
SiH_2Li_2 (4s)	2.251		
CH_2Li_2 (as 3s)[c]		2.175[c]	0.109[c]
CH_2Li_2 (as 4s)[c]		2.213	0.128
SiH_2Na_2 (3s(Na))	10.315		

[a] Minimum in the projected electron density function along the Si–Li or C–Li bond, e au^{-2}. [b] Reference 22. [c] Reference 4b.

Disodiosilanes. To extend this study further, three singlet and four triplet structures of disodiosilane were optimized at the 3-21G level (Table VI, Figure 4). The overall structural patterns are remarkably similar to those of the dilithiosilanes. The structure **3s(Na)** is the global singlet minimum, with the conventional tetrahedral geometry. The structure **1s(Na)**, corresponding to the **1s** in dilithiosilane, is only 2.4 kcal mol^{-1} above **3s(Na)** at 3-21G//3-21G. No local minimum could be found with the inverted tetrahedral C_{2v} structure. On the triplet potential surface, on the other hand, **1t(Na)** corresponds to **1t** and **3t(Na)** corresponds to **3t**. No local minimum with structure similar to **4t** was found. Other minima, **5t(Na)**-$^3B_1$ and **6t(Na)**-$^3B_1$, with geometries similar to their lithium counterparts, are 6.6 and 4.5 kcal mol^{-1} higher in energy than the **1t(Na)**-$^3B_2$.

For direct comparison of the dilithio- and disodiosilanes with their carbon counterparts, we consider the geometry and energy trends among the singlet tetrahedral (3s), triplet tetrahedral (1t), singlet planar cis (4s), and triplet planar cis (6t) structures; all

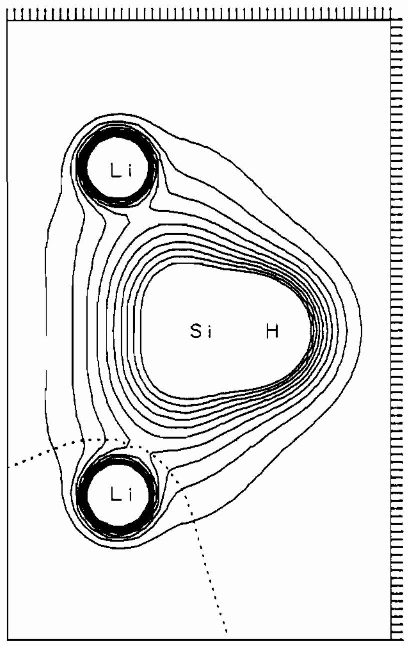

Figure 6. Projected electron density for the $SiLi_2$ plane of singlet "tetrahedral" SiH_2Li_2 (**3s**) with contour levels from 0.02 to 0.2 by 0.02 e au^{-2} at 6-31G*.

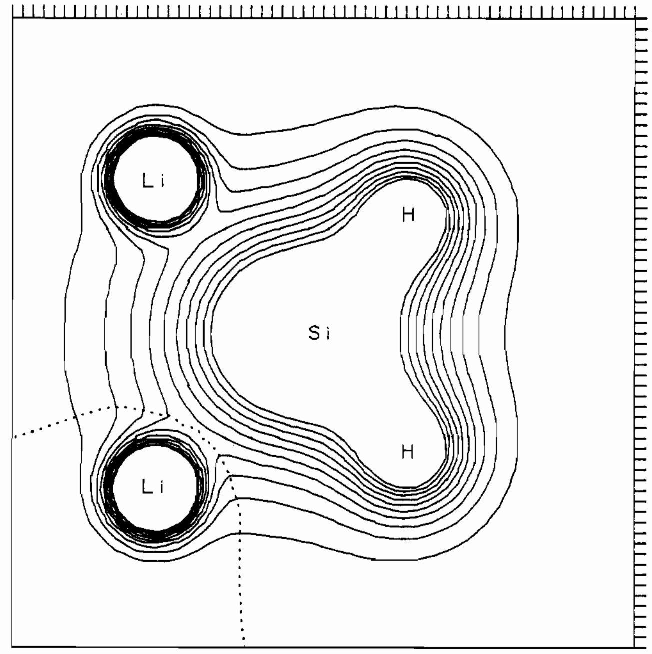

Figure 7. Projected electron density of singlet planar *cis*-SiH_2Li_2 (**4s**) with contour levels from 0.02 to 0.2 by 0.02 e au^{-2} at 3-21G.

are reminiscent of dilithiomethanes.[4] The Si–Li (Si–Na) bond length increases along the series 4s, 3s, 6t, and 4t. These bonds are shorter in singlets than in triplets and in planar compared to tetrahedral structures. The LiSiLi (NaSiNa) angles decrease along the series 3s, 4s, 1t, and 6t. Hence, the longer silicon–metal bonds in the triplets are associated with smaller angles. All of these trends are similar to those in the carbon counterparts (CH_2Li_2). As discussed above, the change from the singlet to the triplet states can be achieved by promotion of an electron from the singlet HOMO to the a_1 LUMO. The singlet HOMO contributes to M–Si bonding, to M–M antibonding for the tetrahedral geometry, and to some M–M bonding for the planar geometry. Thus, this promotion results in loss of M–Si bonding and lengthening of the M–Si distance together with a reduction in the M–M distance. The M–Si–M angle necessarily reduces. The energy difference between the planar cis and the tetrahedral dilithiosilane singlets (**4s**–**3s**, 22 kcal mol^{-1}) is larger than that for the dilithiomethanes (7.3 kcal mol^{-1} at 6-31G**). The trans singlet planar dilithiosilane isomer (**6s**, D_{2h}) lies 80.5 kcal mol^{-1} (3-21G//3-21G(*)) above **3s**. *trans*-CH_2Li_2 (D_{2h}), on the other hand, is 47 kcal mol^{-1} higher in energy than the tetrahedral form at 4-31G.[4a] Because of the favorable electrostatic interactions between the lithiums and the hydrogens, the singlet trans structure, **5a** (C_{2v}), is only 10.7 kcal mol^{-1} (MP2/6-31G*//3-21G(*) + ZPVE) above **3s**. As with the dilithiomethanes, the trans isomer of triplet planar dilithiosilane (**7t**-$^3B_1$) is relatively less favorable than the cis isomer (**6t**).

Ionicity of Silicon–Lithium and Silicon–Sodium Bonds. The integrated projected electron populations (IPP) were calculated for several 3-21G and 6-31G* optimized structures for silyllithium, silylsodium, tetrahedral dilithiosilane (**3s**), planar dilithiosilane (**4s**), and tetrahedral disodiosilane **3s(Na)**. These structures were chosen for direct comparison with the carbon analogues.[4,21] The silicon–alkali-metal bond is only marginally less ionic than the carbon–lithium bond (Table VI), despite the higher electronegativity of carbon compared to silicon. The minimum of the projected electron density for the Si–Li bond is even smaller than that for the C–Li bond (Table VI, Figures 6 and 7) undoubtedly because of the longer Si–Li bond length. The alkali-metal IPP increases in the order $LiSiH_3$ < **3s** < **4s**, which corresponds to the behavior of their carbon counterparts (Table VI).

These results show that the bonding and electronic structures in singlet dilithio- and disodiosilanes are in many aspects rather similar to those in the corresponding dilithiomethanes.[4] The energy difference between the planar and tetrahedral geometries for the dilithiomethane singlets can be modeled by the methylene dianion and two lithium cations. There is a significant difference in the analogous model involving the silylene dianion. The charge distribution in the model silylene dianion differs substantially from that in the methylene dianion because of the strong $Si^{\delta+}H^{\delta-}$ polarization of the Si–H bonds.[18] This effect leads to structures (such as **1s**, **2s**, and **5s**) in which lithium cations and hydrogens are in proximity. Such bridging of hydridic hydrogens by a lithium cation is found in silyllithium, where the inverted tetrahedral structure has been calculated to be the global minimum.[8] The triple-ion character of these structures leads to flat potential energy surfaces, as also found for related dilithiocarbon systems.[22]

The situation for the triplet is analogous although some of the silylene dianion charge is shifted toward the lithiums or sodiums. Consequently, metal–metal bonding becomes an important structural feature. For example, triplet geometries with close Li–H rather than Li–Li contacts, such as **3t**, **4t**, and **7t**, are relatively high in energy. Thus, **7t** cannot form a partial Li–Li bond as in the cis form. The low-lying triplet states can be visualized as a union of a silylene radical anion and a dilithium radical cation. This is underscored by the fact that **1t**-$^3B_2$, **6t**-$^3B_2$, and **5t**-$^3B_1$, which have different orientations of the dilithium radical cation with respect to the silylene fragment, are almost degenerate. The remarkable dipole moment of 12 D for **5t** might result in its stabilization in highly polar condensed media. Structures such as **4t** and **2t** represent a compromise between Li–Li bonding and Li–H bridging.

We note that planar singlet cis dilithiosilane (**4s**) has a π-symmetric HOMO (b_1) analogous to its carbon counterpart.[5b] Lithium substitution in silane causes a dramatic change in the electronic structure for the planar geometry, since the d-symmetric (a_1 for C_{2v}) HOMO in SiH_4 is replaced by a π-symmetric (b_1 for C_{2v}) HOMO. Consequently, the predictions of the importance of d orbitals and π-donating–σ-accepting substituents in the stabilization of planar tetracoordinate silanes[7] are not applicable to substitution by strongly electropositive groups. In fact, dilithio-

(21) (a) For the geometry of CH_3Li at various theoretical levels, see: Kaufman, E.; Raghavachari, K.; Reed, A. E.; Schleyer, P. v. R. *Organometallics* **1988**, *7*, 1597. (b) Streitwieser, A., Jr.; Williams, J. E., Jr.; Alexandratos, S.; McKelvey, J. M. *J. Am. Chem. Soc.* **1976**, *98*, 4778. (c) Schiffer, H.; Ahlrichs, R. *Chem. Phys. Lett.* **1986**, *124*, 172.

(22) Rajca, A.; Streitwieser, A., Jr.; Tolbert, L. M. *J. Am. Chem. Soc.* **1987**, *109*, 1970.

and disodiosilanes exhibit small calculated energy differences between planar and tetrahedral geometries for tetracoordinate silicon, as expected for what are essentially triple ion clusters.[23]

Conclusion

The lowest singlet and triplet potential energy surfaces for dilithiosilanes and disodiosilanes are very flat, as expected for effectively triple-ion clusters. Polarization at silicon, the hydridic character of the hydrogens (SiH_2), and, in the triplets, metal–metal bonding contribute to the existence of rather unusual structures.

Acknowledgment. We dedicate this paper to Professor Hans Bock on the occasion of his 60th birthday. This work was supported at Berkeley in part by AFOSR Grant 82-0114 and by NSF Grants CHE85-02137 and 87-21134 and at Erlangen by the Deutsche Forschungsgemeinschaft, the Fonds der Chemischen Industrie, and Convex Computer Corp. The Berkeley–Erlangen collaboration was also facilitated by a NATO grant. We thank A. J. Kos and J. A. Pople for preliminary calculations on this problem, A. E. Reed for discussions, and H. Xie for technical assistance.

(23) Streitwieser, A., Jr. *Acc. Chem. Res.* **1984**, *17*, 353.

Notes

Contribution from the Dipartimento di Chimica Inorganica e Struttura Molecolare, Università di Messina, 98100 Messina, Italy, and Department of Chemistry, University of Sheffield, S3 7HF Sheffield, England

NMR Investigation of the Rh_2^{4+} Complex $Rh_2(form)_2(O_2CCF_3)_2(H_2O)_2$ (form = *N,N'*-Di-*p*-tolylformamidinate) in the Presence of Phosphorus Donors. Evidence for the Interconversion from the Axial to Equatorial Adducts

Enrico Rotondo,† Brian E. Mann,‡ Pasquale Piraino,*,† and Giuseppe Tresoldi†

Received November 23, 1988

Complexes containing the Rh_2^{4+} core are of significance from the theoretical point of view as well as for their potential catalytic and carcinostatic activity.[1] Until recently the chemistry of this class of compounds has been limited to principally the presence of four carboxylate groups as bridge ligands while their reactivity with Lewis bases appeared to be restricted to the free axial sites. The substitution of the carboxylate groups by other bridging monoanionic ligands in the "lantern structure"[2] was shown to dramatically affect the redox potentials of these species but not their chemical reactivity, which is still restricted to the formation of axial adducts (class I according to the Andersen description).[3a] Recently, Drago et al. reported that the trifluoroacetate derivative $Rh_2(O_2CCF_3)_4$ reacts with nitrogen donor ligands such as *tert*-butyl isocyanide and pyridine giving 1:4 adducts.[4] In these adducts the neutral ligands are coordinated both axially and equatorially (class III) with the trifluoroacetate, exhibiting mono- and bidentate coordination. Furthermore, it was shown that the complexes $Rh_2(O_2CCF_3)_4L_2$ [L = PPh_3, $P(C_6H_{11})_3$], which belong to class I in the solid state, exist in solution as a mixture of axial and axial–equatorial adducts.[4b] Among the $M_2(carboxylate)_4$ (M = Rh, Mo) complexes, only the fluoroalkanecarboxylate-substituted systems lead to the formation of equatorial adducts. It thus appears that the formation of equatorial adducts is dependent on the presence of good leaving groups.

Recently we reported the synthesis of the Rh_2^{4+} complex $Rh_2(form)_2(O_2CCF_3)_2(H_2O)_2$ (form = *N,N'*-di-*p*-tolylformamidinate) in which the trifluoroacetate groups are in a position trans to the formamidinate ligands.[5] This should lead to the weakening of the Rh–O bond and enhance the chemical reactivity of the fluorocarboxylate groups. The reaction between the complex $Rh_2(form)_2(O_2CCF_3)_2(H_2O)_2$ and the phosphorus donors PPh_3, $P(C_6H_{11})_3$, $PMePh_2$, PMe_2Ph, $P(Bu^n)_3$, $P(Bu^t)_3$, $P(OMe)_3$, PPh_2H, and PMe_3 has now been investigated by NMR spectroscopy, and where possible the products were isolated.

† Università di Messina.
‡ University of Sheffield.

Experimental Section

$Rh_2(form)_2(O_2CCF_3)_2(H_2O)_2$ was prepared by the literature procedure.[5] The phosphorus ligands were all obtained from commercial suppliers and were used without further purification. Infrared spectra were recorded on KBr pellets with a Perkin-Elmer 783 instrument. The NMR spectra were measured in $CDCl_3$ by using a Bruker WP-80SY spectrometer for ^{19}F and some ^{31}P and a WH-400 spectrometer for ^{1}H, ^{13}C, ^{103}Rh, and some ^{31}P spectra. The chemical shifts are referenced to Me_4Si for ^{1}H and ^{13}C, $CFCl_3$ for ^{19}F, and external 85% H_3PO_4 for ^{31}P (high frequency is taken as being positive). Elemental analysis were performed by the Analytische Laboratorien Malissa and Reuter, Elbach, West Germany. All the reactions were carried out under nitrogen.

Synthesis of the Complexes $Rh_2(form)_2(O_2CCF_3)_2L$. The reactions were all carried out in a similar manner. The following procedure is typical. To a solution of $Rh_2(form)_2(O_2CCF_3)_2(H_2O)_2$ (0.12 g, 0.13 mmol) in $CHCl_3$ was added the phosphorus ligand (mole ratio 1:1). The resultant solution was stirred for 30 min at room temperature. After this time, *n*-heptane was added, affording, by slow evaporation of the solvent, the monoadducts.

L = PPh_3. Red crystals formed, yield 80%. Anal. Calcd for $Rh_2C_{52}H_{45}N_4O_4F_6P$: C, 54.75; H, 3.97; N, 4.91; P, 2.71. Found: C, 54.95; H, 4.11; N, 4.93; P, 2.70. Infrared spectrum (KBr pellet, cm^{-1}): $\nu_{asym}(CO_2)$ 1635 (s); ν(N⩦C⩦N) 1570 (s). ^{103}Rh NMR ($CDCl_3$): δ 3394 (dd), 7086 (d, J_{Rh-Rh} = 38.6 Hz).

L = $P(C_6H_{11})_3$. Red crystals formed, yield 85%. Anal. Calcd for $Rh_2C_{52}H_{63}N_4O_4F_6P$: C, 53.89; H, 5.48; N, 4.83; P, 2.67. Found: C, 54.14; H, 5.39; N, 4.85; P, 2.75. Infrared spectrum (KBr pellet, cm^{-1}): $\nu_{asym}(CO_2)$ 1640 (s); ν(N⩦C⩦N) 1570 (s). ^{13}C NMR ($CDCl_3$): δ 34.1 (d, CH, J_{P-C} = 18 Hz), 29.0 (s, CH_2), 27.4 (d, CH_2, J_{P-C} = 9 Hz), 26.1 (s, CH_2), 114.4 (s, CF_3), 112.9 (s, CF_3), 147.1, 125.4, 130, and 134.1 (ipso, ortho, meta, and para carbons), 147, 124.7, 129.7, and 134.1 (ipso, ortho, meta, and para carbons), 146.2, 123.7, 129.2, and 133.2 (ipso, ortho, meta, and para carbons), 146, 122.6, 129, and 133 (ipso, ortho, meta, and para carbons), 171.3 (s, CO_2), 168.8 (s, CO_2).

L = $P(Bu^t)_3$. Green crystals formed, yield 85%. Anal. Calcd for $Rh_2C_{46}H_{59}N_4O_5F_6P$: C, 50.28; H, 5.41; N, 5.09; P, 2.81. Found: C, 49.46; H, 5.14; N, 4.96; P, 3.85. Infrared spectrum (KBr pellet, cm^{-1}): $\nu_{asym}(CO_2)$ 1660 (s); ν(N⩦C⩦N) 1575 (s).

L = $P(Bu^n)_3$. Dichroic green-red crystals formed, yield 75%. Anal. Calcd for $Rh_2C_{46}H_{57}N_4O_4F_6P$: C, 51.12; H, 5.31; N, 5.18; P, 2.86. Found: C, 51.38; H, 5.38; N, 5.09; P, 2.90. Infrared spectrum (KBr pellet, cm^{-1}): $\nu_{asym}(CO_2)$ 1660 (s); ν(N⩦C⩦N) 1570 (s). ^{1}H NMR ($CDCl_3$): δ 0.71 (d, PCH_3, J_{P-H} = 10 Hz). ^{13}C NMR ($CDCl_3$): δ 25.6 (d, CH_2, J_{P-C} = 7 Hz), 24.6 (d, J_{P-C} = 10 Hz), 20.8 (d, J_{P-C} = 7 Hz), 13.4 (s, CH_3), 112.9 (s, CF_3), 151.3, 126.5, 129.5, and 134.4 (ipso, ortho,

(1) (a) Cotton, F. A.; Walton, R. A. *Multiple Bonds between Metal Atoms*; Wiley-Interscience: New York, 1982; p 311. (b) Felthouse, T. R. *Prog. Inorg. Chem.* **1982**, *20*, 109. (c) Boyer, E. B.; Robinson, S. D. *Coord. Chem. Rev.* **1983**, *50*, 109.
(2) Piraino, P.; Bruno, G.; Lo Schiavo, S.; Laschi, F.; Zanello, P. *Inorg. Chem.* **1987**, *26*, 2205 and references therein.
(3) (a) Girolami, G. S.; Mainz, V. V.; Andersen, R. A. *Inorg. Chem.* **1980**, *19*, 805. (b) Girolami, G. S.; Andersen, R. A. *Inorg. Chem.* **1982**, *21*, 1318.
(4) (a) Telser, J.; Drago, R. S. *Inorg. Chem.* **1984**, *23*, 2599. (b) Telser, J.; Drago, R. S. *Inorg. Chem.* **1986**, *25*, 2992.
(5) Piraino, P.; Bruno, G.; Tresoldi, G.; Lo Schiavo, S.; Zanello, P. *Inorg. Chem.* **1987**, *26*, 91.

0020-1669/89/1328-3070$01.50/0